Towards Modeling Non-Isothermal Sloshing of Liquid Hydrogen

Basilisk (Gerris) Users' Meeting 2025

Jacob Maarek
Institut Jean Le Rond D'Alembert
Sorbonne Université

July 7-9, 2025

Context

HASTA

Hydrogen Aircraft Sloshing Tank Advancement

Funded by
the European Union

Funded by the European Union (HASTA, 101138003). Views and opinions expressed are however those of the author(s) only and do not necessarily reflect those of the European Union. Neither the European Union nor the granting authority can be held responsible for them.

Context

Goal: Develop a hydrogen tank design tool for the civil aeronautical industry

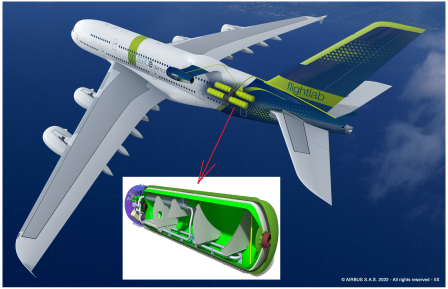

Mockup of A380 with LH2 Fuel Tank

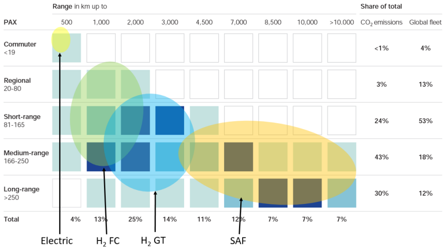

Impact of Renewable Aviation Technologies on CO2 emissions

Context

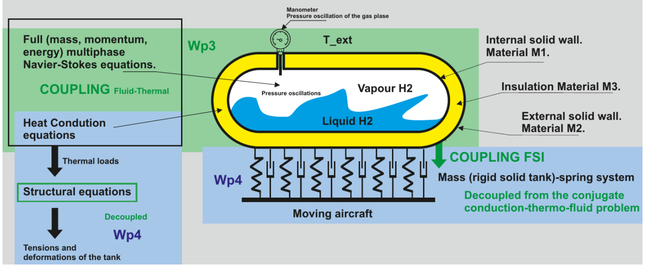

System diagram of LH2 tank

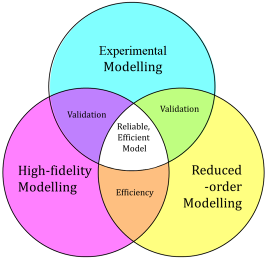

Subprojects of HASTA

Overview

Physical Phenomena Present in Cryogenic Sloshing Tank

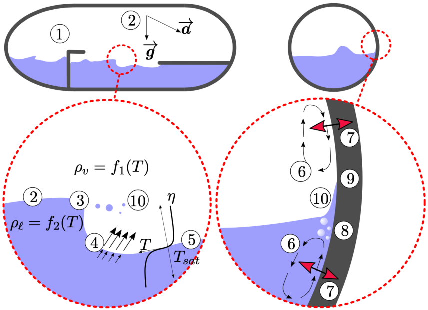

1. Sloshing physics (isothermal) in a complex tank geometry
2. Consistent numerical modeling of gravity and tank acceleration for multiphase flow
3. Densities in both phases are sensitive to temperature variations
4. Phase change effects, including the interface velocity jump (Stefan flow) and calculation of the mass transfer rate
5. High Jakob number (Ja $\approx$ 70), leading to thin thermal boundary layers
6. Natural convection driven boundary layers (Re $\approx 6 \times 10^7$, Ra $\approx 3 \times 10^9$)
7. Coupled solid-fluid heat transfer
8. Nucleate boiling
9. Dynamic contact line in super-heated wall with very small contact angles
10. Phase change at small length scales, like droplets and films

Schematic representation of tank and flow physics to be modelled

Large range of length/time scales

Slosh Induced Pressure Drop

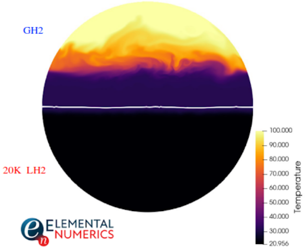

Temperature distribution in two-phase system

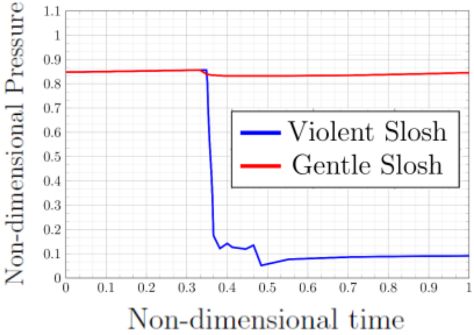

Gentle Slosh → Stratification → Slow/No Pressure Drop
Violent Slosh → Mixing → Fast Pressure Drop

Gas Nondimensional Numbers

$$Pr \approx 0.7$$

$$Ra = Pr\frac{g\rho_0^2(T_h - T_c)L^3}{T_0\mu^2} \approx 10^9$$

$$\epsilon = \frac{T_h - T_c}{T_h + T_c} \approx 0.66$$

$$M \approx 0.01 \text{ (slosh velocity)}$$

Thermal compressible effects must be considered

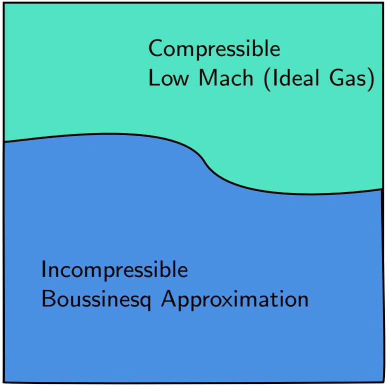

Low mach solver used in gas phase

Numerical Capabilities: Not Exhaustive!

Problem	Numerical technique	Sandbox
Navier-Stokes Eqs.	Incompressible (liquid) Low-Mach (gas)	centered.h jmaarek/two_phase_low_mach.h
Fluid-Solid Interaction	Moving Reference Frame Embed+VOF	tavares/contact-embed.h
Turbulence Modeling	LES	Antoonvh/vreman.h
Conjugate Heat Transfer	Time-implicit flux-partioned diffusion	Antoonvh/diffusion-pair.h jmaarek/diffusion-three_field.h
Phase Change	Interface Velocity-Jump	ecipriano/
Thin Thermal BL	BL-SGS	maarek/thin_BL/

Liquid Equations Solved: Boussinesq Incompressible NS

$$\rho \frac{d\mathbf{u}}{dt} = -\nabla \cdot (\rho \mathbf{u} \otimes \mathbf{u}_{rel}) + \left[-\nabla p' + \nabla \cdot \left(2\mu \left[\nabla \mathbf{u} + (\nabla \mathbf{u})^T \right] \right) \right] + \mathbf{F}_\sigma + \mathbf{g} \cdot \mathbf{x} \nabla \rho \tag{1}$$

$$\nabla \cdot \mathbf{u} = 0 \tag{2}$$

$$\partial_t f + \mathbf{u}_{rel} \cdot \nabla f = 0 \tag{3}$$

$$\mathbf{u} = \mathbf{u}_{rel} + \mathbf{u}_{rigid} \qquad \mathbf{u}_{rigid} = \mathbf{u}_{trans} + \Omega \times \mathbf{r} \tag{4}$$

$$\rho c_p \frac{\partial T}{\partial t} + \rho c_p (\mathbf{u}_{rel} \cdot \nabla T) = \nabla \cdot (k \nabla T) \tag{5}$$

Gas Equations Solved: Conservative Low Mach Equations

$$\rho \frac{d\mathbf{u}}{dt} = -\nabla \cdot (\rho \mathbf{u} \otimes \mathbf{u}_{rel}) + \left[-\nabla p' + \nabla \cdot \left(2\mu \left[\nabla \mathbf{u} - (\nabla \mathbf{u})^T - \frac{2}{3} (\nabla \cdot \mathbf{u}) \mathbf{I} \right] \right) \right] + \mathbf{F}_\sigma + \mathbf{g} \cdot \mathbf{x} \nabla \rho \tag{6}$$

$$\cancel{\overline{P} = \rho R T} \tag{7}$$

$$\frac{d\overline{P}}{dt} = (\gamma - 1) \int_V \nabla \cdot (k \nabla T) \, dV \tag{8}$$

$$\frac{\partial (\rho h)}{\partial t} + \nabla \cdot (\rho \mathbf{u}_{rel} h) = \nabla \cdot (k \nabla T) + \frac{d\overline{P}}{dt} \tag{9}$$

$$\nabla \cdot \mathbf{u} = \frac{R}{\overline{P} c_p} \left(\nabla \cdot (k \nabla T) - \frac{1}{\gamma - 1} \frac{d\overline{P}}{dt} \right) - \frac{\zeta}{\gamma \overline{P}} \frac{\rho R T - \overline{P}}{\Delta t} \tag{10}$$
[1,2]

[1] J. Bell, "Amr for low mach number reacting flow," in *Adaptive Mesh Refinement-Theory and Applications: Proceedings of the Chicago Workshop on Adaptive Mesh Refinement Methods, Sept. 3–5, 2003*, pp. 203–221, Springer

[2] R. Knikker, "A comparative study of high-order variable-property segregated algorithms for unsteady low mach number flows," *International Journal for Numerical Methods in Fluids*, vol. 66, no. 4, pp. 403–427, 2011

VOF + Embed

- tavares/contact-embed.h [3]
- easily generalisable to 3D
- Fixed problem of orientation-dependent numerical pinning (zero volumetric flux)

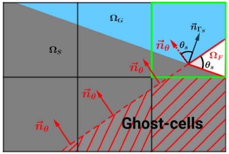

VOF extrapolation with contact angle

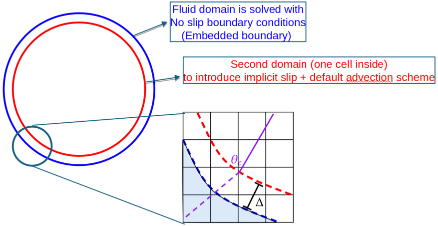

Modification: Perform extrapolation from boundary one cell inside fluid domain

[3] M. Tavares, C. Josserand, A. Limare, J. M. Lopez-Herrera, and S. Popinet, "A coupled vof/embedded boundary method to model two-phase flows on arbitrary solid surfaces," *Computers Fluids*, vol. 278, p. 106317, 2024

VOF + Embed Validation 1: Sessile Drop Inclined Plane

tavares/test_cases/sessile_embed.c

Validation performed by Theo Witkamp

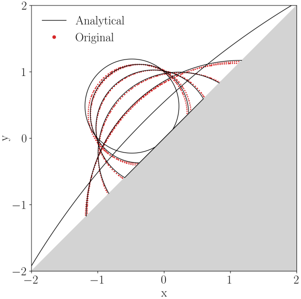

Original

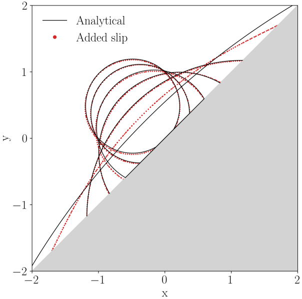

Modified

Better agreement for steady state position, even at shallow angles

VOF + Embed Validation 1: Sessile Drop Inclined Plane

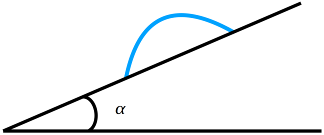

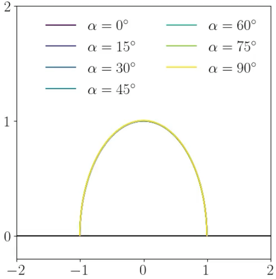

Original

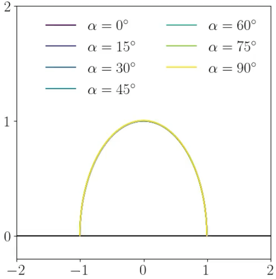

Modified

Orientation dependent spreading error signficantly improved

VOF + Embed Validation 2: Sessile Drop Inclined Plane 3D

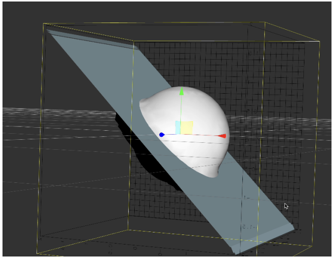

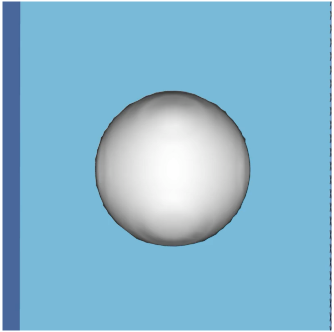

Original

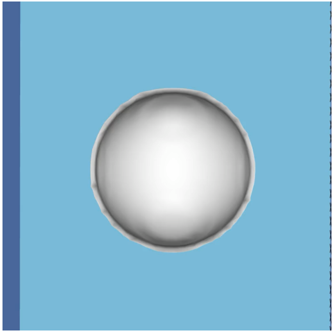

Modified

3D asymmetry removed with modification

Low Mach Validation 1: Heated Cavity Benchmark Case

$\mathrm{Ra} = 10^7$, $\epsilon = 0.6$, Sutherland's law for viscosity, conductivity, maxlevel 9

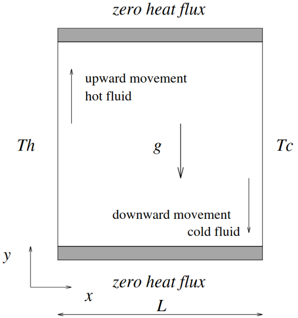

Benchmark schematic [4]

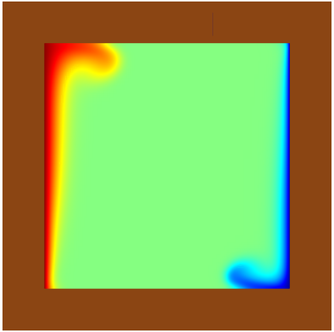
Temperature distribution

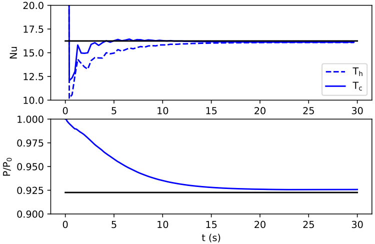

Nusselt Number, Pressure Evolution

[4] Le Quéré, Patrick, Weisman, Catherine, Paillère, Henri, Vierendeels, Jan, Dick, Erik, Becker, Roland, Braack, Malte, and Locke, James, "Modelling of natural convection flows with large temperature differences: A benchmark problem for low mach number solvers. part 1. reference solutions," *ESAIM: M2AN*, vol. 39, no. 3, pp. 609–616, 2005

Low Mach Validation 2: GH2 Passive Pressurisation

Heated at 3.5 $\mathrm{W/m^2}$ for 2 hrs, Sutherland's law for viscosity, conductivity

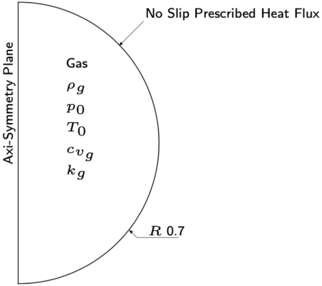

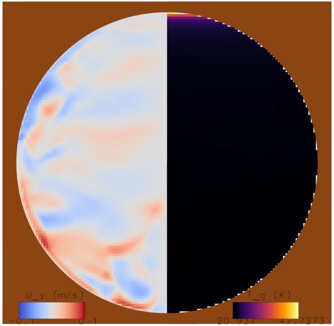

Y-velocity, Temperature

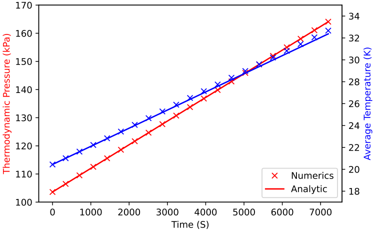

Pressure evolution $\frac{dP}{dt} = (\gamma - 1)\frac{Q}{V}$

Isothermal Sloshing 1: Rectangular Domain

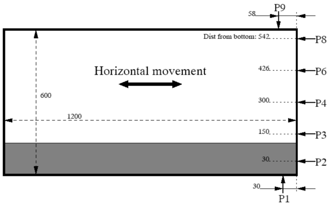

Numerical Benchmark schematic [5]

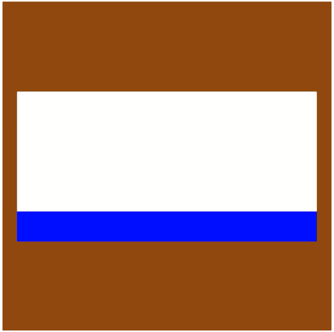

Interface Deformation

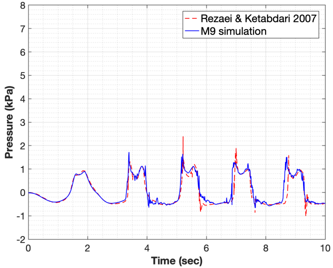

Pressure signal at probe P1

[5] H. Rezaei and M. J. Ketabdari, "Numerical modelling of sloshing with vof method," in *The 12th International Conference on Fluidization - New Horizons in Fluidization Engineering* (F. Berruti, X. T. Bi, and T. Pugsley, eds.), (London, Canada), ECI Symposium Series, 2007

Isothermal Sloshing 2: Circular Domain

Air-Water system, corresponding experiments published in [6]

Simulations performed by Pavan Kumar Kirar

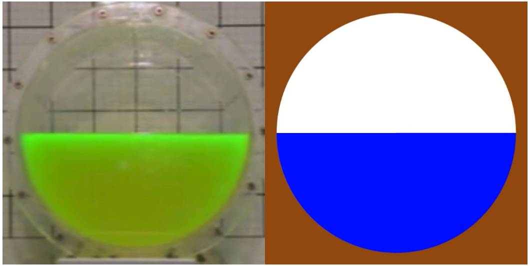

1 Hz $f/f_N \approx 0.8$

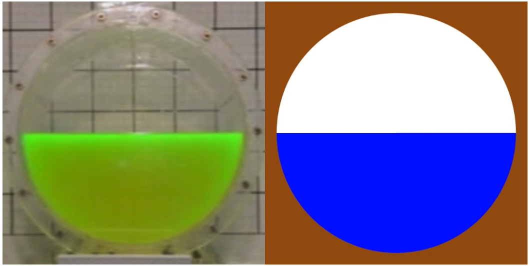

1 Hz $f/f_N \approx 0.96$

[6] Ángel Luis Martín López, *Estudio Teórico Experimental de la Estabilidad Lateral en Vehículos Cisterna. Metodología para la Determinación del Umbral de Vuelco*. Phd thesis, Universidad Politécnica de Madrid, Escuela Técnica Superior de Ingenieros Industriales, Madrid, Spain, 2013

Isothermal Sloshing 2: Circular Domain

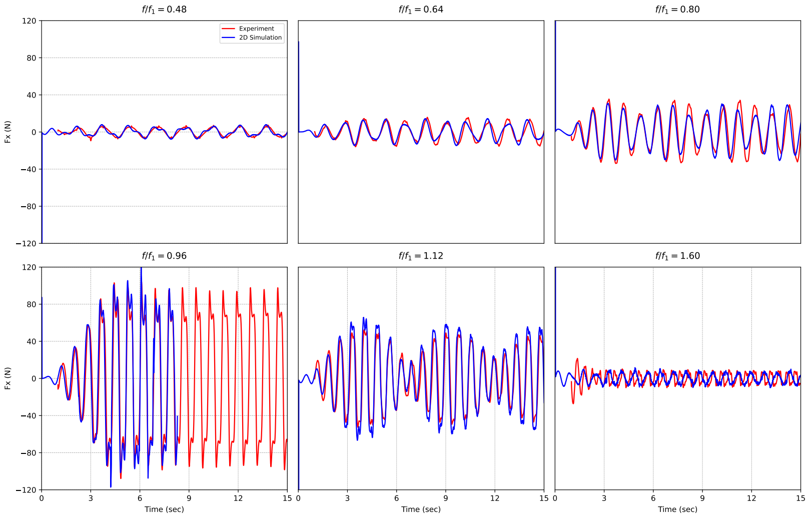

Parametric study of X-force response compared with experiment

Isothermal Sloshing 3: Horizontal Cylinder, Roll Excitation

Horizontal cylinder with rounded ends [7]

Air-Water system, compared with unpublished COMSOL simulations, maxlevel 9

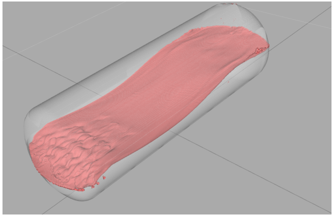

View of fluid interface, tank

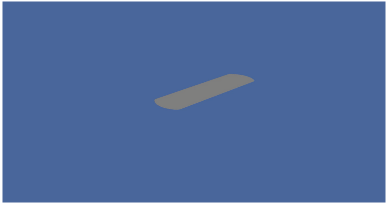

Interface Deformation f = 0.4Hz

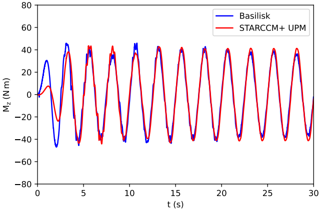

Torque at axis of rotation

[7] E. L. Grotle and V. Æsøy, "Numerical simulations of sloshing and the thermodynamic response due to mixing," *Energies*, vol. 10, no. 9, 2017

Conclusion

1. Proposed simple correction to existing VOF+Embed that significantly reduces orientation-dependent contact-line mobility
2. Developed, validated low-mach solver for gas phase
3. Performed 2D/3D isothermal sloshing simulations, relatively good agreement observed for measured forces

Next Steps

1. Perform 2-phase NASA self-pressurisation test case [8]
2. Include phase-change, non-ideal effects
3. Perform non-isothermal slosh simulations, validation with published numerical simulations [9], LH2 experiments performed by group members

[8] W. L. Johnson, L. M. Ameen, F. D. Koci, D. Oberg, and J. G. Zoeckler, "Structural heat intercept, insulation and vibration evaluation rig (shiiver)," in *Proceedings of Space Propulsion 2018*, (Seville, Spain), p. –, NASA Glenn Research Center / European Space Agency / 3AF, May 2018. Report No. SP-2018-179 (GRC-E-DAA-TN54730)

[9] E. L. Grotle and V. Æsøy, "Numerical simulations of sloshing and the thermodynamic response due to mixing," *Energies*, vol. 10, no. 9, 2017